DOI: 10.1002/ejic.200900059

Self-Association of [Pt^{II}(1,10-Phenanthroline)(*N*-pyrrolidyl-*N*-(2,2-dimethylpropanoyl)thiourea)]$^+$ and Non-Covalent Outer-Sphere Complex Formation with Fluoranthene through π–Cation Interactions: A High-Resolution ^{1}H and DOSY NMR Study

Izak A. Kotzé,[a] Wilhelmus J. Gerber,[a] Jean M. Mckenzie,[a] and Klaus R. Koch*[a]

Keywords: Noncovalent interactions / Pi interactions / NMR spectroscopy / Diffusion coefficients / Association constants

Competing outer-sphere self-association of [Pt^{II}(1,10-phenanthroline)(*N*-pyrrolidyl-*N*-(2,2-dimethylpropanoyl)thiourea)]$^+$ Cl^- (M) and the hetero-association of M with fluoranthene (F) have been investigated by means of the significant concentration dependence of ^{1}H NMR chemical shifts as well as by diffusion coefficients obtained from DOSY NMR spectroscopy. The NMR spectroscopic data is only consistent with the formation of a "dimer" M···M aggregate according to $2M \rightleftharpoons M_2$ in acetonitrile at several temperatures, with a calculated K_D of ca. 46 ± 7 M^{-1} at 273.5 K. In the presence of the aromatic molecule fluoranthene, relatively strong, presumably π–cation-type interactions between M and F according to $M + F \rightleftharpoons MF$ ($K_B \approx 67 \pm 7$ M^{-1} at 273.5 K) occur in acetonitrile. The calculated $\Delta_r H°$ and $\Delta_r S°$ for M···M (-25129 ± 3112 and -61 ± 11 J mol^{-1}) and M···F (-13560 ± 3180 and -17 ± 11 J mol^{-1}, respectively) is indicative of π–cation interactions. Interestingly any potential F···F aggregation interactions are negligible for the fluoranthene concentration range up to 0.1 M, indicating that non-covalent π–π interactions between fluoranthene molecules $2F \rightleftharpoons F_2$ are, in contrast to π–cation interactions, negligible under these conditions in solution.

Introduction

Non-covalent π–cation interactions have been the subject of extensive interest in the last decade in view of their well established role and importance in biological systems[1–5] as well as in supra-molecular chemistry and molecular recognition phenomena.[3,6–8] There are several manifestations of this type of non-covalent bonding interaction, the simplest and most extensively studied system involves group I and II metal cations or protonated amine with benzene and other aromatic molecules in the gas and solution phase.[2,9] The detailed nature of π–cation interactions have been reviewed and in the *gas phase* for example, the K^+···benzene interaction energies can exceed K^+···H_2O interaction,[10,11] and it has been convincingly shown that "organic" cations, such as ammonium ions, can strongly interact with suitably designed synthetic arene-based receptors as well as in numerous biological structures.[12,13] In aqueous solution, cations are obviously solvated resulting in the attenuation of the π–cation interaction leading to elongation of the interaction distance between the cation and arene centre as compared to such interactions in the gas phase.[9] In the case of "stacking" and/or aggregation of metalloporphyrins, Hunter and Sanders[14] derived an elegant simple electrostatic model which demonstrate that so-called "π–π" interactions in planar metalloporphyrins actually arise from favourable π–σ attractions which overcome π–π repulsions in such molecules. This model has resulted in a set of rules with which to predict the nature and relative interaction geometry of such aggregation phenomena, at least in the case of planar metalloporphyrins.

We have become interested in the chemistry of planar, formally cationic mixed-ligand Pt^{II} complexes of the general structure [Pt(diimine)(L-*S*,*O*)]$^+$ (where diimine is 2,2′-bipyridine or 1,10-phenanthroline and HL-*S*,*O* represents various chelating *N*-acyl-*N*,*N*′-dialkylthioureas) which have been shown to display interesting biological activity ranging from significant potential anti-malarial activity,[15a] to interesting DNA intercalation with demonstrable in vivo activity toward bacterial *E. coli* AB1886 (*uvr A*) cultures;[15b] moreover preliminary work shows that such complexes undergo some interesting DNA-mediated biomineralization.[16] We have previously studied a series of [Pt^{II}(diimine)(L-*S*,*O*)]PF_6 salts which were found to display well defined aggregation behaviour in acetonitrile solutions, which we ascribed to π–cation interactions leading to the formation of non-covalent "dimer aggregates" in solution.[17] For this system we found that the Gibbs free energy associated with the "dimer aggre-

[a] Department of Chemistry and Polymer Science, University of Stellenbosch,
Private Bag X1, Matieland, 7602 Stellenbosch, South Africa
Fax: +27-21-808-3342
E-mail: krk@sun.ac.za

Supporting information for this article is available on the WWW under http://www.eurjic.org or from the author.

gates" formation increases by approximately 2.4 kJ mol^{-1} per aromatic ring of the diimine bound to Pt^{II}; these Gibbs free energies are slightly higher than energies reported by Rebeck et al. for only "π–π stacking" interactions of 1.8 kJ mol^{-1}.[18]

By contrast to the well known group I and II metal cations and protonated amine systems which show significant π–cation interactions[2,9] outer-sphere complexes with uncharged aromatic molecules by means of π–cation or combinations of π–cation and π–π stacking interactions with planar complex cations such as $[Pt^{II}(diimine)(L\text{-}S,O)]^+$ and even $[Pt^{II}(diimine)_2]^{2+}$ have received comparatively little attention in the literature.[6,17,19] The in vitro anti-malarial activity of $[Pt^{II}(diimine)(L\text{-}S,O)]^+$ is postulated to arise by inhibition of β-hematin (synthetic hemozoin or malaria pigment) formation in view of the cationic Pt^{II} complexes forming moderately strong outer-sphere complexes with ferriprotoporphyrin IX in 40% aqueous dimethyl sulfoxide (DMSO) solution.[15]

In this context, we examined potential π–cation interactions between the $[Pt^{II}(phen)(L\text{-}S,O)]^+Cl^-$ complex (Scheme 1) and fluoranthene ($C_{16}H_{10}$) in acetonitrile as a model system, by means of ^{1}H NMR concentration-dependence studies as well as Diffusion Ordered Spectroscopy (DOSY) to probe these phenomena. ^{1}H NMR is particularly well suited for this type of investigation because the relevant thermodynamic parameters can be estimated from the concentration dependence of ^{1}H chemical shifts,[19–21] while the relative spatial orientation of the complex cation within an aggregate in solution can be inferred.[17] DOSY experiments[3] have been used as an independent method to estimate the thermodynamic properties of this system[3,20] and to obtain estimated hydrodynamic volumes of aggregates, which gives a measure of the number of molecules present in an "aggregate".[22,23] This model system is representative of competing non-covalent π–cation interactions leading to self-association of the complex $[Pt^{II}(phen)(L\text{-}S,O)]^+$ cation on the one hand, and π–cation interactions between fluoranthene and the complex in solution, on the other.

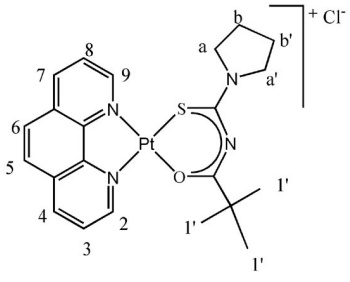

Scheme 1. Structure and numbering scheme for $[Pt^{II}(phen)(L\text{-}O,S)]^+Cl^-$.

Computational Methods

In the model system examined in this work, several simultaneous chemical equilibria may be present. From the average observed signal response, $X_{obsd.}$, equation (1) (where X_i = ^{1}H chemical shift, δ_i, or diffusion coefficient, D_i, and a_i = mole fraction of species i) and the total concentration of reagents, we want to calculate for the reactions defined in a chemical model the equilibrium constant(s), K_i, and chemical shifts, δ_i, or diffusion coefficients, D_i, of individual species (dimer aggregates, trimer aggregates, ion-pairs, etc).

$$X_{obsd.} = \sum_{i=n} a_i X_i \quad (1)$$

This particular type of mathematical problem can be solved in several ways.[24] We opted to use a program called, DIMER-K_D, written by us several years ago to fit data with a dimerization model[17] (the program utilizes the algorithm by Horman and co-workers[21]). When dealing with multiple equilibria we used a program called Dynafit version 3[25] that is freely available for academic purposes. The signal response that Dynafit version 3 can handle is however slightly different from equation (1); instead of using mole fraction in equation (1), Dynafit uses the concentration of the species, c_i. This problem was circumvented by multiplying equation (1) with the total concentration, C_T, of the reagent of interest and after grouping terms, equation (2) is obtained.

$$C_T X_{obsd.} = \sum_{i=n} c_i X_i \quad (2)$$

Results and Discussion

Self-Association of $[Pt^{II}(phen)(L\text{-}S,O)]^+$ in Acetonitrile

Figure 1 illustrates ^{1}H NMR spectra obtained as a function of $[Pt^{II}(phen)(L\text{-}S,O)]^+$ concentration at 267.1 K in CD_3CN. The marked concentration dependence of the chemical shift of particularly the H^2 and H^9 signals of the coordinated 1,10-phenanthroline moiety suggests that self-association/aggregation processes are occurring with increasing concentration, as we have previously demonstrated for related complexes.[17] Moreover, the spectra reveal that whatever aggregated species exist in solution are in fast-exchange (in chemical shift) on the NMR time-scale, because only sharp ^{1}H resonances for all protons on the complex are observed over the concentration and temperature ranges studied. Significantly, *all* the ^{1}H resonances of the 1,10-phenanthroline group show differing degrees of $\delta_{obsd.}$ concentration dependence, depending on their relative positions in the 1.10-phenanthroline ring system (Supporting Information, Figure S1), while the chemical shifts of the protons of the coordinated *N*-pyrrolidyl-*N*-(2,2-dimethylpropanoyl)thiourea ligands show a much smaller concentration dependence. Possible dissociation reactions of the $[Pt^{II}(Phen)(L\text{-}S,O)]^+$ complex over time, such as Cl^- coordination to the Pt^{II} metal centre following chelate ring-opening reactions, may be excluded because no spectral changes consistent with dissociation are observed over a 5 d period at any fixed concentration for the temperature range 278–301 K.

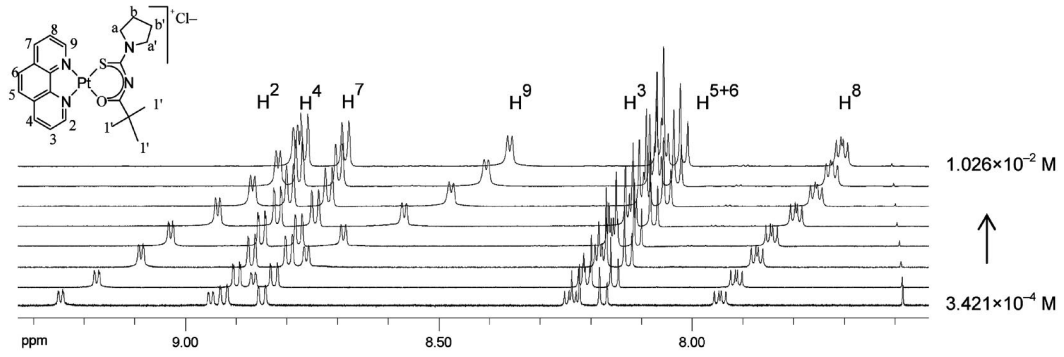

Figure 1. ^{1}H NMR spectra (599.99 MHz) of $[Pt^{II}(phen)(L\text{-}S,O)]^+$ in CD_3CN at 273.4 K with increasing complex concentration. Only a partial spectrum is shown as several nuclei (*N*-pyrrolidyl-*N*-(2,2-dimethylpropanoyl)thiourea protons) exhibit no or little chemical-shift concentration dependence.

Several intermolecular processes in solution may be invoked to account for the concentration dependence of the $\delta_{obsd.}$, notably self-association or aggregation of $[Pt^{II}(phen)(L\text{-}S,O)]^+$ cations and/or ion-pairing between the complex cation and Cl^- ion (due to the relatively low dielectric constant of acetonitrile, $k \approx 36$, at 298 K). We postulate that the concentration dependence of the $\delta_{obsd.}$ for the $[Pt^{II}(phen)(L\text{-}S,O)]^+Cl^-$ salt in acetonitrile solution is due essentially to "dimer aggregate" (D) formation consisting of two planar complex $[Pt^{II}(phen)(L\text{-}S,O)]^+$ cations participating in π–cation stacking interaction in solution (vide infra). Self-association of $[Pt^{II}(phen)(L\text{-}S,O)]^+$ leading to higher order aggregates such as a "trimer" or even "tetramer" aggregates would result in more highly charged species which are unlikely in acetonitrile. Nonetheless, to critically examine our postulate of the formation of only dimer aggregates, as well as to exclude the possibility of ion-pairing and/or higher order aggregates being present in solution, we attempted to fit various models including dimer, trimer, and tetramers, as well as a model in which $[Pt^{II}(phen)(L\text{-}S,O)]^+\cdots Cl^-$ ion-pairing occurs, to the data shown in Figure 2 using non-linear least-squares regression methods. With the exception of the simple dimer (D) model, relation (3), all other models however resulted in absurdly large relative percentage error for calculated equilibrium constants associated with possible ion-pairing and/or higher than dimer self-association processes, disqualifying such more complicated models.

The excellent fit between the $\delta_{obsd.}$ and calculated values obtained with only the dimer (D) model shown in Figure 2 [see also equation (4)] and further, the plausible calculated chemical shifts of the monomer and dimer of the H^2 protons (9.316 ± 0.029 and 7.851 ± 0.089 ppm, respectively, at 299.2 K) provide a compelling argument for only the dimer model postulated here. Using this model, where M = $[Pt^{II}(phen)(L\text{-}S,O)]^+$ monomer and M_2 = $[Pt^{II}(phen)(L\text{-}S,O)]^+$ dimer, "dimerization" constants (K_D) and chemical shifts (δ_i) for the relevant protons were estimated to within a 95% confidence limit for each temperature, while the relative percentage error for all parameters are below 13% at worst (Table 1).

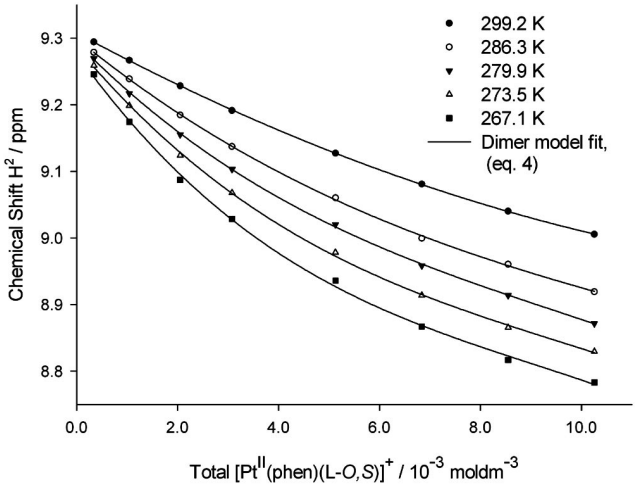

Figure 2. Excellent agreement was obtained between the dimer model least-squares fits and the experimental (symbols) chemical-shift dependence of the 1,10-phenanthroline H^2 proton on the concentration of $[Pt^{II}(phen)(L\text{-}S,O)]^+$.

$$2M \overset{K_D}{\rightleftharpoons} M_2 \quad (3)$$

$$C_{T(Pt)}\delta_{obsd.} = c_M\delta_M + 2c_{M2}\delta_{M2} \quad (4)$$

Table 1. Calculated dimerization constants, K_D for $[Pt^{II}(phen)(L\text{-}O,S)]^+$ in CD_3CN and thermodynamic data.

Temp [K]	K_D [M^{-1}]	$\Delta_rH°$ [J mol^{-1}]	$\Delta_rS°$ [J mol^{-1}]	$\Delta_rG°$ [J mol^{-1}]
299.2	17 (± 2)	–25129 (± 3112)	–61 (± 11)	–6998
286.3	27 (± 5)			–7777
279.9	29 (± 3)			–8167
273.5	46 (± 7)			–8556
267.1	56 (± 8)			–8946

As the temperature is raised from 267.1 to 299.2 K, the $K_D = 56 \pm 7$ M^{-1} decreases to 17 ± 2 M^{-1}, indicating as expected that dimer formation is exothermic. The standard reaction enthalpy, $\Delta_rH°$, and entropy, $\Delta_rS°$, can be estimated by fitting the Van't Hoff equation (5) to the temperature-dependent K_D data. Over the relatively small tempera-

ture range used here (Δ 32.1 K), it is expected that the $\Delta_r H°$ and $\Delta_r S°$ are temperature independent yielding a linear plot of $\ln(K_D)$ vs. T^{-1}. This is confirmed by the good linear trend obtained using the Van't Hoff equation (Figure 3), which further validates the dimer aggregate model; the standard reaction enthalpy (slope) and entropy (intercept) of reaction 3 are listed in Table 1. The relatively large, negative $\Delta_r S°$ is indicative of an association reaction consistent with the inference that only dimer aggregates are formed. By comparison, ion-pair processes are typically associated with a positive $\Delta_r S°$ changes, as solvated molecules are "released" upon ion-pair formation.[3,26] Furthermore, it is clear from the thermodynamic data (Table 1) ($\Delta_r H° < 0$, $T\Delta_r S° < 0$) that the dimer-formation reaction is enthalpy driven and that this thermodynamic behaviour is indicative of π–cation binding.[3]

$$\ln(K_D) = -\frac{\Delta_r H°}{RT} + \frac{\Delta_r S°}{R} \quad (5)$$

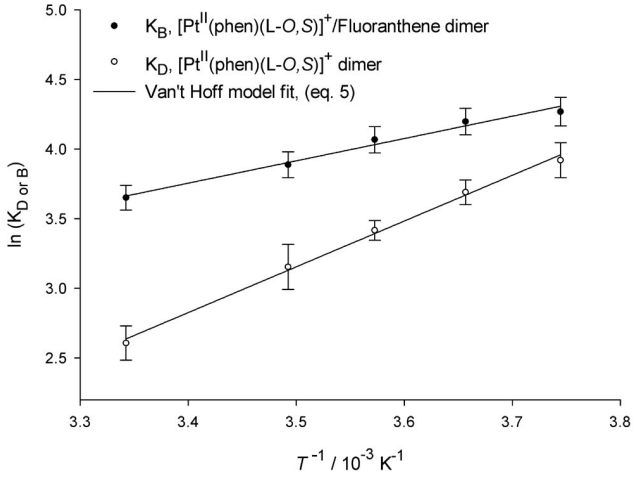

Figure 3. The good linear fits obtained with the Van't Hoff equation is further validation for the self- and hetero-association (vide infra) of $[Pt^{II}(phen)(L\text{-}O,S)]^+$ and fluoranthene in CD_3CN. The 95% confidence interval of the slopes and intercepts for the $[Pt^{II}(phen)(L\text{-}O,S)]^+$ and $[Pt^{II}(phen)(L\text{-}O,S)]^+$/fluoranthene dimers equal 3287.8 (± 374.2)x –8.4 (±1.3) and 1602.9 (± 383.0)x –1.7 (±1.4), respectively.

Given the relatively simple dimer model, it is reasonable to expect that molecular diffusion processes might be affected by increased dimer formation, as a function of increasing complex concentration. This expectation is confirmed by diffusion-ordered ^{1}H NMR spectroscopy (DOSY) which we show here to be an independent method with which to verify conclusions drawn from the concentration and temperature ^{1}H NMR chemical-shift dependence studies. Experiments with diffusion-delay times varying from 30 to 200 ms resulted in no significant differences in DOSY spectra nor in calculated diffusion coefficients (DOSY spectrum Supporting Information Figure S3); it is therefore reasonable to conclude that only an averaged diffusion coefficient, $D_{obsd.}$, is observed.[27] Unlike the ^{1}H-chemical-shift experiments discussed above, all protons of the complex $[Pt^{II}(phen)(L\text{-}S,O)]^+$ in equilibrium with the dimer yield the "same" diffusion coefficient and this method is therefore not dependent on the individual proton chemical shifts. The D_{CD_3CN} obtained here (39.5×10^{-10} m^2 s^{-1}) differs by less than 7% from the value obtained by Kato and coworkers[28] (4.3×10^{-9} m^2 s^{-1}), and consequently we used the D_{CD_3CN} as an internal "standard". The $D_{obsd.}$ for the complex is proportional to the sum of the product of the individual diffusion coefficients, D_i, and the concentration of the species (i) present [equation (6)]. Estimation of the K_D from diffusion data are based on the same mathematical algorithm[21] as for the ^{1}H-chemical-shift dependence described above.

$$C_{T(Pt)}D_{obsd.} = c_M D_M + 2c_{M2}D_{M2} \quad (6)$$

As the concentration of $[Pt^{II}(phen)(L\text{-}S,O)]^+$ increases experimental diffusion coefficients decrease (Figure 4), consistent with a dimer model. The least-squares fit with the dimerization model (relation 6) is in good agreement with the diffusion data (Figure 4) and the calculated K_D from diffusion data at 299.2 K is 15 ± 8 M^{-1} (ΔG = –6737 J mol^{-1}). This compares well with the K_D calculated from the chemical shift data 17 ± 2 M^{-1} (ΔG = –7048 J mol^{-1}) and supports the simple dimer model. The agreement is reasonably acceptable given that the relative percent error of measured diffusion coefficients is at best 4%, albeit much larger than the relative percentage error in the measurement of a ^{1}H NMR chemical shift (0.2%), arguably leading to a less precise value of K_D from DOSY NMR spectroscopic data (Figure 4). The satisfactory agreement between the two differing ways of estimating K_D indicates that this model is internally consistent.

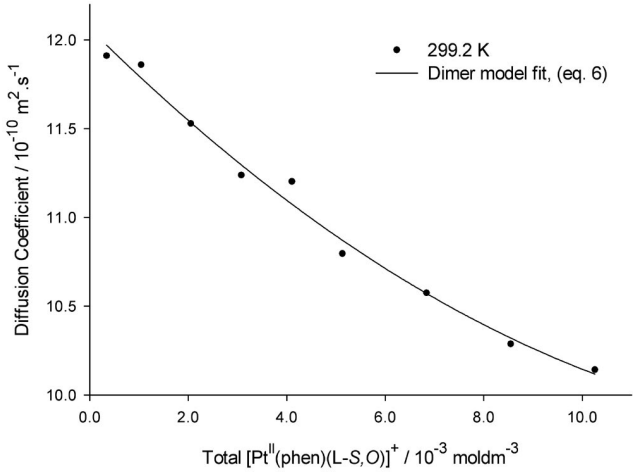

Figure 4. Good agreement was obtained between the dimer model least-squares fit and the experimental (symbols) diffusion-coefficient dependence on the concentration of $[Pt^{II}(phen)(L\text{-}S,O)]^+$ at 299.2 K.

In principle the hydrodynamic radius and volume of a complex may be estimated from DOSY data at a given concentration, because the diffusion coefficient is related to molecular size by the well known Stokes–Einstein equation

(7), from which the hydrodynamic radius, r_H, and volume, V_H, of the molecules/aggregates in question can be estimated,

$$D = \frac{kT}{6\pi\eta r_H} \quad (7)$$

where k is the Boltzmann constant, T is the absolute temperature and η the solvent viscosity.[22] This equation assumes a spherical molecule and is obviously a rather crude approximation of our square-planar complexes. We assumed that the solvent viscosity does not change significantly with solute concentration, which is justified for the relatively low solute concentrations used and by the negligible change in D_{CD_3CN} values ($39.53 \pm 0.72 \times 10^{-10}$ m^{2}s^{-1}) obtained for all solutions of differing solute concentration examined at 299.2 K. The hydrodynamic radii estimated (Table 2) from the $D_{obsd.}$ represents an "average" of the monomer and dimer. From the least-squares fit of the data in Figure 4, the [Pt^{II}(phen)(L-*S*,*O*)]$^+$ monomer and dimer individual diffusion coefficients were estimated at ca. $12.1 \pm 0.6 \times 10^{-10}$ and $5.9 \pm 0.8 \times 10^{-10}$ m^{2}s^{-1}, respectively from which the hydrodynamic radii for the monomer and dimer could be estimated to be 4.8 (± 2.3) and 10.1 (± 3.5) Å, respectively. The r_H value for the [Pt^{II}(phen)(L-*S*,*O*)]$^+$ complex is reasonable when compared to the $r_{H,X\text{-ray}}$ estimated from single-crystal X-ray data of two crystal structures,[29,30] which is 5.8 Å (Supporting Information Diagram S1), whereas the calculated r_H of the dimer is reasonable when considering two [Pt^{II}(phen)(L-*S*,*O*)]$^+$ species in close contact.

Table 2. Diffusion coefficients D ($\times 10^{-10}$ m^{2}s^{-1}), hydrodynamic radii r_H [Å] and hydrodynamic volumes V_H (Å^3) for [Pt^{II}(phen)(L-*O*,*S*)]$^+$ in CD_3CN at different complex concentrations [mM].

Concentration [mM]	D [10^{-10} m^{2}s^{-1}]	r_H [Å]	V_H [Å^3]
10.26	10.14 (± 0.07)	5.82	824.1
8.55	10.29 (± 0.09)	5.73	789.6
6.84	10.58 (± 0.08)	5.58	726.8
5.13	10.80 (± 0.11)	5.46	683.2
4.10	11.20 (± 0.11)	5.27	611.5
3.08	11.24 (± 0.13)	5.25	605.6
2.05	11.53 (± 0.17)	5.12	561.0
1.04	11.86 (± 0.12)	4.97	515.2
0.34	11.91 (± 0.18)	4.95	508.7

The consistency of the DOSY data with that obtained from the concentration dependence of the $\delta_{obsd.}$(^{1}H) of the [Pt^{II}(phen)(L-*S*,*O*)]$^+$ complex is convincing support of dimer formation through π–cation association of these planar Pt^{II} complexes. Unfortunately, numerous attempts to obtain crystals suitable for single crystal X-ray diffraction failed to date, so that direct structural support for the geometrical nature of the dimer aggregate is lacking at present. Nevertheless, from the ^{1}H-chemical-shift trends observed (Figure 1) it is possible to infer a most likely structure of the dimer aggregate. The relatively small concentration dependence of the $\delta_{obsd.}$ for the butyl and *N*-pyrrolidyl protons compared to the relatively large concentration dependence of the chemical shift of the 1,10-phenanthroline protons (H^2 and H^9), suggests that these complexes stack *regiospecifically* in a face-to-face manner involving the phenanthroline sides of the complex. An unlikely "T-shaped" edge-on geometry[14] for the dimer can be ruled out given the chemical shift trends observed (Supporting Information, Figure S1). Such a coplanar stacking arrangement will maximize the π–cation attractions and minimize π–π repulsion to result in an offset π–cation stacking geometry between adjacent complexes consistent with related metalloporphyrins suggested by the Sanders[14] model as in Scheme 2. Depicted in the scheme are the most reasonable dimer aggregate structures postulated in solution; because the system is in fast exchange in chemical shift, only an average structure can be proposed from NMR spectroscopic data in view of several possible geometric stacking interactions conceivable.

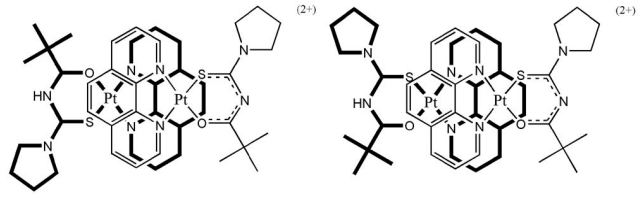

Scheme 2. Proposed average [Pt^{II}(phen)(L-*S*,*O*)]$^+$ dimer aggregate structures in solution.

Non-Covalent Association of [Pt^{II}(phen)(L-*S*,*O*)]$^+$ and Fluoranthene

Addition of small quantities of aromatic molecules such as fluoranthene ($C_{16}H_{10}$) to a solution of [Pt^{II}(phen)(L-*S*,*O*)]$^+$ in acetonitrile, leads to changes in the ^{1}H NMR spectrum of the complex (Figure S2), resulting in significant shielding of H^2 and H^9 protons of the [Pt^{II}(phen)(L-*S*,*O*)]$^+$ cation in proportion to the relative mole ratio of [Pt^{II}-(phen)(L-*S*,*O*)]$^+$ to fluoranthene. Such behaviour suggests substantial non-covalent association between fluoranthene and the [Pt^{II}(phen)(L-*S*,*O*)]$^+$ complex, through π–cation interactions. Because only single resonances for all ^{1}H of the [Pt^{II}(phen)(L-*S*,*O*)]$^+$ complex are observed at these temperatures in solution, the system is in fast exchange in chemical shift as observed for the self-association of the [Pt^{II}(phen)(L-*S*,*O*)]$^+$ described above. We have investigated this phenomenon quantitatively by means of the concentration dependence of the ^{1}H resonances ($\delta_{obsd.}$) of the platinum complex as a function of added fluoranthene, with the view of estimating the association constants between the π-electron-rich fluoranthene and the planar complex cation in acetonitrile. With the addition of fluoranthene (F) to a solution of [Pt^{II}(phen)(L-*S*,*O*)]$^+$ in acetonitrile, the simplest additional reactions to aggregation of the complex cation (M), are the aggregation of fluoranthene itself to form at least a fluoranthene dimer (F_2) – see equation (8) – and outer-sphere complex formation between M and F, through π–cation interactions, see equation (9).

$$2F \overset{K_A}{\rightleftharpoons} F_2 \quad (8)$$

$$M + F \overset{K_B}{\rightleftharpoons} MF \quad (9)$$

To test if fluoranthene undergoes aggregation in acetonitrile (equation 8), the concentration dependence of the ^1H chemical shift was studied in the temperature range 266 to 298 K. Changes in ^1H chemical shifts of fluoranthene were found to be very small (relative to the data in Figure 2) resulting in a total Δ 0.015 ppm over the range of 1.05 mM to 0.1 M fluoranthene. The relatively poor solubility of fluoranthene in acetonitrile prevented examination of higher concentrations, and hence precluded a reliable estimate of an aggregation (of at least dimer formation) constant from this data, so that we reasonably estimate a $K_A < 0.1\ M^{-1}$ at 266 K. Such a K_A value implies that the mole fraction of un-associated fluoranthene (α_F) is > 0.98 at the highest practical fluoranthene concentration of 0.1 M. Clearly any π–π stacking of fluoranthene in acetonitrile can be taken to be essentially negligible in a total concentration range up to 0.1 M fluoranthene achievable in [D_3]acetonitrile.

Addition of increasing amounts of fluoranthene to an acetonitrile solution containing a constant amount of [Pt^{II}-(phen)(L-*S*,*O*)]$^+$ (7.62 mM) caused a considerable change in the chemical shift of the H^2 and H^9 protons of 1,10-phenanthroline (Figure 5a). To initially simplify matters, we assumed that only self- and hetero-noncovalent dimer formation (relations 3 and 9) occur. Therefore, the $\delta_{obsd.}$ change of the H^2 and H^9 protons of 1,10-phenanthroline in the Pt^{II} complex as a function of increasing fluoranthene concentration can be expressed by equation (10), where M = [Pt^{II}-(phen)(L-*S*,*O*)]$^+$ monomer, M_2 = [Pt^{II}(phen)(L-*S*,*O*)]$^+$ dimer and MF = [Pt^{II}(phen)(L-*S*,*O*)]$^+$/fluoranthene dimer.

$$C_{T(Pt)}\delta_{obsd.} = c_M\delta_M + 2c_{M2}\delta_{M2} + c_{MF}\delta_{MF} \quad (10)$$

If the addition of fluoranthene only caused the dissociation of the [Pt^{II}(phen)(L-*S*,*O*)]$^+$ dimer in some manner and hence increased the [Pt^{II}(phen)(L-*S*,*O*)]$^+$ monomer concentration, c_M, the $\delta_{obsd.}$ change of the H^2 proton (Figure 5a) should undergo de-shielding. The data in Figure 5a clearly show the converse, indicating significant [Pt^{II}-(phen)(L-*S*,*O*)]$^+$/fluoranthene non-covalent aggregate formation (relation 9). Confirmation of [Pt^{II}(phen)(L-*S*,*O*)]$^+$ and fluoranthene non-covalent association can be obtained by analyzing the fluoranthene H^{2*} proton chemical-shift data (Figure 5b). The change in the $\delta_{obsd.}$ of the H^{2*} proton of fluoranthene as a function of increasing fluoranthene concentration may be expressed by equation (11), where F = fluoranthene and MF = [Pt^{II}(phen)(L-*S*,*O*)]$^+$/fluoranthene complex.

$$C_{T(F)}\delta_{obsd.} = c_F\delta_F + c_{MF}\delta_{MF} \quad (11)$$

Increasing concentration of fluoranthene leads to de-shielding of H^{2*} of fluoranthene after which the extent of de-shielding levels off (Figure 5b), in contrast to when no [Pt^{II}(phen)(L-*S*,*O*)]$^+$ is present in solution. The relative concentration ratio of MF to F determines whether the $\delta_{obsd.}$ [equation (11)] is relatively more shielded or de-shielded. The concentration ratio of MF to F is largest when the total fluoranthene concentration is lowest, so that as the total fluoranthene concentration increases, the concentration ratio decreases, resulting in the monomer term ($c_F\delta_F$) contributing relatively more to the $\delta_{obsd.}$ with each addition of fluoranthene so resulting in progressive de-shielding of the H^{2*} proton (Figure 5b). The concentration dependence of the fluoranthene chemical shift data is thus consistent with [Pt^{II}(phen)(L-*S*,*O*)]$^+$/fluoranthene aggregation.

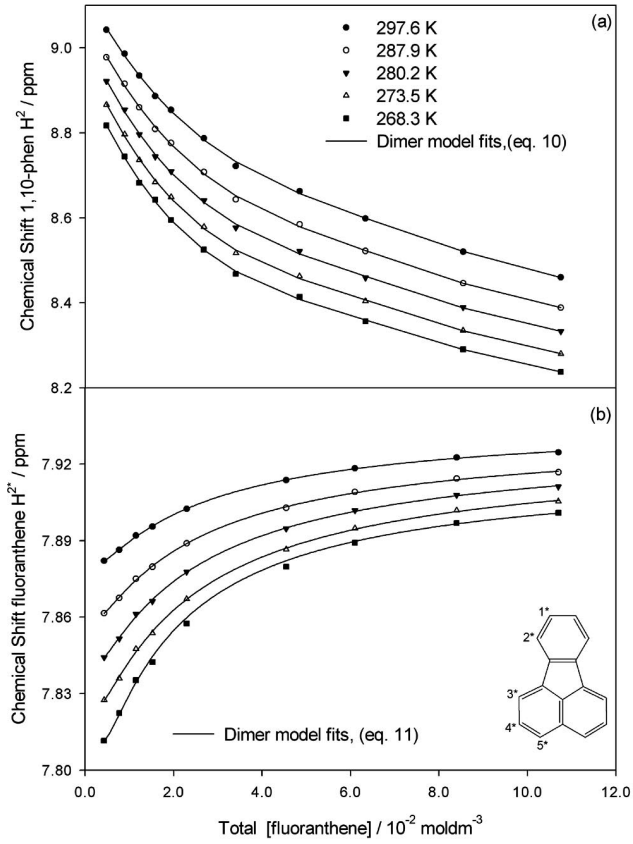

Figure 5. Excellent agreement was obtained between the experimental (symbols) chemical shift dependence of (a) the 1,10-phenanthroline H^2 proton and (b) the fluoranthene H^{2*} proton as a function of fluoranthene concentration and the self- and hetero-association dimer model least-squares fits.

The least-squares fit of the self- and hetero-association model (relations 3 and 9) to the proton chemical-shift data (see parts a and b in Figure 5) at several temperatures are in excellent agreement with the experimental data. When fluoranthene self-association (relation 8) is included in the least-squares model fit the program Dynafit only converged with K_A values very close to zero confirming that the extent of possible fluoranthene dimerization is *negligible* compared to reactions 3 and 9 (Figure 6).

Thermodynamic data for the self- and hetero-association model (relations 3 and 9) are obtained by the good fit with the Van't Hoff equation (5) (Figure 3), from which the standard reaction enthalpy and entropy of the [Pt^{II}-(phen)(L-*S*,*O*)]$^+$/fluoranthene π–cation interaction was estimated (Table 2). The $\Delta_rS°$ of relation M + F⇌MF (9) is

negative, suggesting association between reactants. It is clear from the thermodynamic data (Table 3) that this hetero-association reaction is also enthalpy driven, indicative of π–cation binding.[3] Comparing the thermodynamic parameters (Table 1 and Table 3) of the self- and hetero-association reactions 3 and 9, reveal that the $[Pt^{II}(phen)(L\text{-}S,O)]^+$/fluoranthene non-covalent complex has a more favourable standard reaction Gibbs energy ($\Delta_rG°$). This may be qualitatively attributed to the absence of charge repulsion present in the self-association interaction of $[Pt^{II}(phen)(L\text{-}S,O)]^+$ cations. The π–cation interaction is however crucial for these non-covalent complexes to form as it is demonstrated here that fluoranthene self-association is negligible under these reaction conditions.

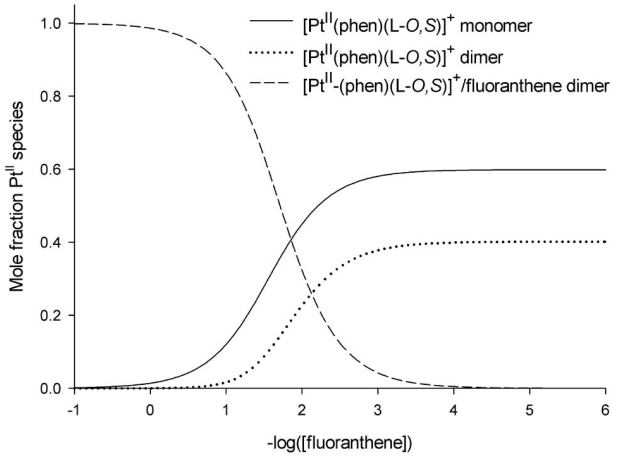

Figure 6. Species distribution diagram when increasing amounts of fluoranthene is added to a Pt^{II} solution, with determined constants K_D and K_B of 56 (±13) M^{-1} and 72 (±7) M^{-1}**, respectively at 267.1 K. Fluoranthene π–π stacking is negligible in the concentration range below 0.1 M.

Table 3. Calculated dimerization constants, K_B for $[Pt^{II}(phen)(L\text{-}O,S)]^+$/fluoranthene in CD_3CN and thermodynamic data.

Temp. [K]	K_B [M^{-1}]	$\Delta_rH°$ [J mol^{-1}]	$\Delta_rS°$ [J mol^{-1}]	$\Delta_rG°$ [J mol^{-1}]
297.6	39 (±4)	–13560 (±3180)	–17 (±11)	–9111
287.9	49 (±5)			–9265
280.2	58 (±6)			–9388
273.4	67 (±7)			–9496
267.6	71 (±7)			–9588

To sum up, our data is indicative of the fact that only a 1:1 $[Pt^{II}(phen)(L\text{-}S,O)]^+$/fluoranthene π–cation complex is present in our solutions in the concentration range studied. The chemical-shift trends observed as a result of the concentration dependence suggest that the 1:1 π–cation complex has an average structure shown in Scheme 3 in which a fluoranthene stacks *regiospecifically* in a coplanar manner to maximize π–σ attraction and minimize π–π repulsions in an offset stacking geometry, similar to that postulated for $[Pt^{II}(phen)(L\text{-}S,O)]^+$ dimer aggregate as shown in Scheme 1.

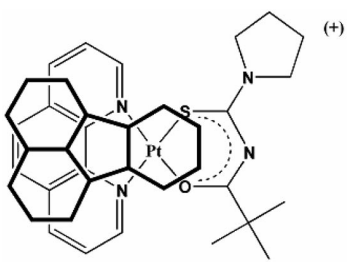

Scheme 3. Proposed average $[Pt^{II}(phen)(L\text{-}S,O)]^+$/fluoranthene dimer aggregate structure in solution.

Conclusions

In conclusion, the ^{1}H-NMR chemical shift and DOSY diffusion-coefficient dependence data of $[Pt^{II}(phen)(L\text{-}S,O)]^+$ validates its self-association into a $[Pt^{II}(phen)(L\text{-}S,O)]^+$ dimer in acetonitrile solutions with K_D (56 ± 8 M^{-1}). Moreover, $[Pt^{II}(phen)(L\text{-}S,O)]^+$ and fluoranthene form a 1:1 π–cation complex with an association constant, K_B (71 ± 8 M^{-1}) larger than the K_D obtained for the self-association of $[Pt^{II}(phen)(L\text{-}S,O)]^+$ into a dimer at 267 K. Higher order aggregates and ion-pairing were found to be negligible on the basis of the excellent least-squares fit of the dimer model to the ^{1}H NMR spectroscopic data and resulting linear Van't Hoff plots. The thermodynamic parameters calculated in this work indicate that π–cation interactions between cationic $[Pt^{II}(phen)(L\text{-}S,O)]^+$ and uncharged aromatic molecules, such as fluoranthene studied here ($\Delta_rG° \approx 9.6$ kJ mol^{-1}), are more favourable than self-association of the $[Pt^{II}(phen)(L\text{-}S,O)]^+$ ($\Delta_rG° \approx 8.9$ kJ mol^{-1}), compared to negligible π–π stacking of fluoranthene in acetonitrile. The data are consistent with essentially coplanar 1:1 aggregate strucrures in solution, resulting from regiospecific stacking interactions. We are currently investigating these phenomena with other model systems in water/acetonitrile mixtures as a step towards understanding the mechanism of anti-malarial activity of $[Pt^{II}(phen)(L\text{-}S,O)]^+$ class of compounds.

Experimental Section

Analytical Instrumentation: ^{1}H NMR and DOSY experiments were done in 5-mm tubes using a Varian Unity Inova 400 MHz spectrometer operating at 399.95 MHz or a Varian Unity Inova 600 MHz spectrometer equipped with an inverse-detection pulsed field gradient (idpfg) probe operating at 599.99 MHz. Diffusion coefficients were extracted using the Varian vnmrj software (version 2.1b). Experimental parameters: Pulse sequence: Dbppste_cc (Bipolar Pulse Pair Stimulated Echo with Convection Compensation), ^{1}H spectral width: 10 ppm, number of acquisitions varied from sample, recycling delay: 2 s, diffusion delay 30 ms, Gradient-pulse duration 2 ms, 20 different values of *G*, the gradient magnitude, varying between 0.0107 and 0.449 G m^{-1}. Melting points were determined using an Electrothermal IA9300 Digital Melting Point Apparatus. UV/Vis spectra were recorded with a single beam Agilent 8253E UV/Vis spectrophotometer. The IR absorbance spectra were recorded with a Thermo Nicolet Nexus FT-IR spectrometer fitted with a Smart-ATR adaptor. C and N were done with an EA Euro 3000 Elemental Analyser. Electro-spray mass spectra were obtained using a Waters API Quattro Micro Mass Spectrometer.

Synthesis of Compounds: All reagents and solvents were commercially available, and were used without further purification. The general method described by Morgan and Burstall for the synthesis of [Pt(1,10-phenanthroline)Cl_2] was used from commercially available $K_2[PtCl_4]$ and 1,10-phenanthroline monohydrate.[31] *N*-(2,2-Dimethylpropanoyl),*N*-pyrrolidylthiourea was prepared as described in the literature.[29] Commercially available fluoranthene (Aldrich) was used without further purification.

[Pt(1,10-phenanthroline)Cl_2]: Yield 201 mg (87.4%), m.p. > 350 °C. ^{1}H NMR (399.95 MHz, [D_6]DMSO, 25 °C): δ = 9.70 [dd, ^4J(H,H) = 1.3, ^3J(H,H) = 5.5 Hz, 2 H, H^9, H^2], 9.04 [dd, ^4J(H,H) = 1.3, ^3J(H,H) = 8.2 Hz, 2 H, H^4, H^7], 8.29 (s, 2 H, H^5, H^6), 8.17 [dd, ^3J(H,H) = 5.5, ^3J(H,H) = 8.2 Hz, 2 H, H^3, H^8] ppm. IR (ATR): $\tilde{\nu}$ = , 3083 (arom. C–H stretch), 3059 (arom. C–H stretch), 1427 (arom. C–C stretch), 1220 (asym. C–N stretch) 1208 (sym. C–N stretch) cm^{-1}. $C_{22}H_{25}ClN_4OPtS$ (624.07): calcd. C 32.3, N 6.3; found C 32.6, N 6.0.

***N′*-(*2,2*-Dimethylpropanoyl),*N*-pyrrolidylthiourea (HL):** Yield 564 mg (90.1%), m.p. 136–137 °C. ^{1}H NMR (399.95 MHz, [D_6]-DMSO, 25 °C): δ = 9.74 (s, 1 H, NH), 3.63 (m, 2 H, H^{a}), 3.42 (m, 2 H, $H^{a'}$), 1.90 (m, 4 H, H^{b}, $H^{b'}$), 1.16 (s, 9 H, $H^{1''}$) ppm. ^{13}C NMR (50.31 MHz, $CDCl_3$, 25 °C): δ = 27.16 ($C^{3''}$), 39.62 ($C^{2''}$), 54.43 ($C^{3'}$), 52.52 (C^3), 26.16 ($C^{4'}$), 24.59 (C^4), 176.66 (C^S), 174.38 (C^O) ppm. UV/Vis: λ_{max} (ε) 216(13 399), 276 nm (14 792 dm^3 mol^{-1} cm^{-1}). $C_{10}H_{18}N_2OS$ (214.33): calcd. C 57.8, H 8.5, N 13.1, S 14.96; found C 57.0, H 8.8, N 13.3, S 14.8.

[*N*-(2,2-Dimethylpropanoyl),*N*-pyrrolidylthiourea](1,10-phenanthroline)platinum(II) Chloride: The general method for the synthesis of mixed-ligand [Pt(diimine)(L-*S*,*O*)]PF_6 described by Koch et al.,[17] was modified for the preparation of [Pt^{II}(phen)(L-*S*,*O*)]Cl. A suspension of [Pt(phen)Cl_2] (0.045 g, 0.1 mmol) in 10 mL of acetonitrile was heated under reflux for 10 min, after which *N*-(2,2-dimethylpropanoyl),*N*-pyrrolidylthiourea (0.022 g, 0.101 mmol) in 2 mL of acetonitrile was added dropwise and the mixture heated under reflux for 45 min. A suspension of sodium acetate (0.028 g, 0.15 mmol) in acetonitrile was added and the mixture was left to gently reflux overnight. The cooled mixture was filtered through Celite to remove any Na/KCl precipitate formed. The filtrate was concentrated by evaporation to volume of ca. 2 mL. Diethyl ether (100 mL) was added and the precipitate was collected by centrifugation, resuspended several times with cold diethyl ether and centrifuged again. The yellow product was dried overnight in a vacuum oven at 70 °C; yield 58 mg (93%), m.p. 134–135 °C ^{1}H NMR (599.99 MHz, CD_3CN): δ = 9.01 [dd, ^4J(H,H) = 0.9, ^3J(H,H) = 4.5 Hz, 1 H, H^2], 8.85 [dd, ^4J(H,H) = 0.9, ^3J(H,H) = 7.7 Hz, 1 H, H^4], 8.77 [dd, ^4J(H,H) = 0.6, ^3J = 7.8 Hz, 1 H, H^7], 8.66 [d, ^3J(H,H) = 5.3 Hz, 1 H, H^9], 8.15 [dd, ^3J(H,H) = 4.5, ^3J(H,H) = 7.7 Hz, 1 H, H^3], 8.12 (m, 2 H, H^5, H^6), 7.84 [dd, ^3J(H,H) = 5.3, ^3J(H,H) = 7.3 Hz, 1 H, H^8] ppm. IR (ATR): $\tilde{\nu}$ = 3086 (arom. C–H stretch), 3059 (arom. C–H stretch), 2969 (C–H stretch), 2927 (C–H stretch), 1482 (C–O stretch), 1380 (CH_3 umbrella deformation), 1434 (arom. C–C stretch) 1264 (asym. C–N stretch) 1228 (sym. C–N stretch) cm^{-1}. (+) ESI MS: *m*/*z* 588 (M^+, calcd. 588.6).

Supporting Information (see also the footnote on the first page of this article): Figure S1 depicts the concentration dependence of the 1,10-phenanthroline protons. Figure S2 illustrates the set of resonance signals for the 1,10-phenanthroline and fluoranthene protons. Figure S3 shows the DOSY plot and the average diffusion coefficient for the aggregating complex. Diagram S1 illustrates how the r_H of [Pt^{II}(phen)(L-*S*,*O*)]$^+$ was estimated from two closely related crystal structures.

Acknowledgments

Financial support from the Stellenbosch University, the National Research Foundation (GUN 2069294) and Angloplatinum Ltd., is gratefully acknowledged.

[1] C. R. Brodie, J. G. Collins, J. R. Aldrich-Wright, *Dalton Trans.* **2004**, *8*, 1145–1152.
[2] D. A. Dougherty, *Science* **1996**, *271*, 163–168.
[3] D. Cuc, D. Canet, J.-P. Morel, N. Morel-Desrosiers, P. Mutzenhardt, *ChemPhysChem* **2007**, *8*, 643–645.
[4] T. Brand, E. J. Cabrita, S. Berger, *Prog. Nucl. Magn. Reson. Spectrosc.* **2005**, *46*, 159–196.
[5] W. Lu, D. A. Vicic, J. K. Barton, *Inorg. Chem.* **2005**, *44*, 7970–7980.
[6] M. Cusumano, M. L. Di Pietro, A. Giannetto, *Inorg. Chem.* **2006**, *45*, 230–235.
[7] A. M. Krause-Heuer, N. J. Wheate, M. J. Tilby, D. G. Pearson, C. J. Ottley, J. R. Aldrich-Wright, *Inorg. Chem.* **2008**, *47*, 6880–6888.
[8] N. J. Wheate, P. G. A. Kumar, A. M. Torres, J. R. Aldrich-Wright, W. S. Price, *J. Phys. Chem. B* **2008**, *112*, 2311–2314.
[9] A. S. Reddy, H. Zipse, G. N. Sastry, *J. Phys. Chem. B* **2007**, *111*, 11546–11553.
[10] J. C. Ma, D. A. Dougherty, *Chem. Rev.* **1997**, *97*, 1303–1324.
[11] J. Sunner, K. Nishizawa, P. Kebarle, *J. Phys. Chem.* **1981**, *85*, 1814–1820.
[12] H. J. Schneider, *Angew. Chem.* **1991**, *103*, 1419–1439.
[13] N. Zacharias, D. A. Dougherty, *Trends Pharmacol. Sci.* **2002**, *23*, 281–287.
[14] C. A. Hunter, J. K. M. Sanders, *J. Am. Chem. Soc.* **1990**, *112*, 5525–5534.
[15] a) T. J. Egan, K. R. Koch, P. L. Swan, C. Clarkson, D. A. Van Schalkwyk, P. J. Smith, *J. Med. Chem.* **2004**, *47*, 2926–2934; b) Y.-S. Wu, K. R. Koch, V. R. Abratt, H. H. Klump, *Arch. Biochem. Biophys.* **2005**, *440*, 28–37.
[16] H. H. Klump, K. R. Koch, C. T. Lin, *S. Afr. J. Chem.* **2006**, *102*, 264–266 .
[17] K. R. Koch, C. Sacht, C. Lawrence, *J. Chem. Soc., Dalton Trans.* **1998**, *4*, 689–695.
[18] J. J. Rebek, *Angew. Chem.* **1990**, *29*, 245–255.
[19] A. Macchioni, A. Romani, C. Zuccaccia, G. Guglielmetti, C. Querci, *Organometallics* **2003**, *22*, 1526–1533.
[20] L. Fielding, *Tetrahedron* **2000**, *56*, 6151–6170.
[21] I. Horman, B. Dreux, *Helv. Chim. Acta* **1984**, *67*, 754–764.
[22] P. S. Pregosin, *Prog. Nucl. Magn. Reson. Spectrosc.* **2006**, *49*, 261–288.
[23] F. Song, S. J. Lancaster, R. D. Cannon, M. Schormann, S. M. Humphrey, C. Zuccaccia, A. Macchioni, M. Bochmann, *Organometallics* **2005**, *24*, 1315–1328.
[24] M. Meloun, J. Havel, E. Högfeldt, *Computation of Solution Equilibria – A Guide to Methods in Potentiometry, Extraction, and Spectrophotometry*, Ellis Horwood, Chichester, **1987**.
[25] P. Kuzmic, *Anal. Biochem.* **1996**, *237*, 260–273.
[26] X.-M. Lu, W.-G. Xu, X.-H. Chang, D.-Z. Lu, J.-Z. Yang, *J. Chem. Thermodyn.* **2006**, *38*, 5–9.
[27] C. S. Johnson, *Prog. Nucl. Magn. Reson. Spectrosc.* **1999**, *34*, 203–256.
[28] H. Kato, T. Saito, M. Nabeshima, K. Shimada, S. Kinugasa, *J. Magn. Reson.* **2006**, *180*, 266–273.
[29] A. N. Mautjana, J. D. S. Miller, A. Gie, S. A. Bourne, K. R. Koch, *Dalton Trans.* **2003**, *10*, 1952–1960.
[30] M. Kato, J. Takahashi, *Acta Crystallogr., Sect. C: Cryst. Struct. Commun.* **1999**, *55*, 1809–1812.
[31] G. T. Morgan, F. H. Burstall, *J. Chem. Soc.* **1934**, 965–971.

Received: January 16, 2009
Published Online: March 18, 2009

